

Synthesis and reactivity of mono(amidinate) organoiron(II) complexes

Timo J. J. Sciarone, Christian A. Nijhuis, Auke Meetsma and Bart Hessen*

Received 7th June 2006, Accepted 11th August 2006

First published as an Advance Article on the web 23rd August 2006

DOI: 10.1039/b608108h

The mono(amidinate) iron(II) ferrate complex $[\{\text{PhC}(\text{NAr})_2\}\text{FeCl}(\mu\text{-Cl})\text{Li}(\text{THF})_3]$ (**1**, Ar = 2,6-*i*Pr₂C₆H₃) was prepared and was found to undergo ligand redistribution in non-coordinating solvents to give the homoleptic $[\{\text{PhC}(\text{NAr})_2\}_2\text{Fe}]$ (**2**) as the only isolable product. Reaction of **1** with alkylating agents also induces this redistribution, but the presence of pyridine allows isolation of the four-coordinate 14 VE monoalkyl complex $[\{\text{PhC}(\text{NAr})_2\}\text{FeCH}_2\text{SiMe}_3(\text{py})]$ (**4**). Generation of the 12 VE alkyl *via* pyridine abstraction from **4** by B(C₆F₅)₃ again induced ligand redistribution. Attempts to trap a 12 VE alkyl species with CO led to the isolation of a dimeric Fe(0)–Li–ferrate complex (**3**) with a carbamoyl ligand, derived from CO insertion into the iron–amidinate bond.

Introduction

Electron-poor (≤ 14 valence electrons (VE)) alkyl complexes of iron are of interest because of their likely involvement in the coordination polymerisation of olefins. Recently, 14 VE cationic Fe(II) monoalkyls supported by a terdentate pyridine-2,6-diimine (PDI) ligand were isolated and were shown to be competent in the catalytic polymerisation of ethene.^{1,2} Nevertheless, definite proof for the nature of the active species in this system remains to be obtained. Thus far, high activity in Fe-catalysed olefin polymerisation has been achieved only using neutral ligands incorporating the PDI skeleton.³

Neutral bidentate ligands have been employed to stabilise Fe(II) dialkyls,^{4,5} but none of these has been reported as a polymerisation catalyst. Also, no highly active catalysts supported by monoanionic ligands have been reported, although various interesting Fe(II) monoalkyls with 14 VE are known.^{6–9} More electron-deficient, three-coordinate Fe(II) monoalkyls (12 VE) have been obtained with β -diketiminate ligands with sterically demanding 2,6-*i*Pr₂C₆H₃ substituents on the nitrogen atoms.^{10,11} These do not display alkene insertion into the Fe–alkyl bond, however, although alkene insertion into the Fe–H bond of the corresponding hydride has been observed.^{10c,d}

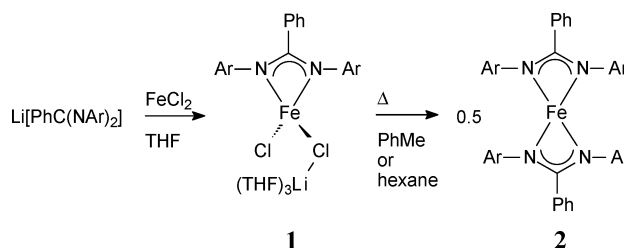
A possible way to enhance the reactivity of these neutral 12 VE systems is to open up the available space around the metal centre by the (conceptual) removal of two carbon atoms from the β -diketiminate NCCCN backbone: this leads to the amidinate ligand framework. Previous studies on the coordination chemistry of bis(amidinate) Fe(II) complexes with sterically demanding benzamidinates $[\text{PhC}(\text{NAr})(\text{NAr}')]\text{Fe}$, (Ar = 2,6-*i*Pr₂C₆H₃, Ar' = Ar, 2,6-Me₂C₆H₃) have shown that the amount of steric congestion imposed by these ligands can have important consequences for the coordination geometry of the resulting Fe(II) complexes.¹²

Here we describe the preparation and reactivity of mono(amidinate) organoiron(II) complexes of the sterically demanding benzamidinate $[\text{PhC}(\text{NAr})_2]\text{Fe}$ (Ar = 2,6-*i*Pr₂C₆H₃).

Reduction of the chelate ring size by two carbons is found to result in organoiron(II) chemistry very distinct from that of the related β -diketiminate ligands.

Results and discussion

Reaction of equimolar amounts of $\text{Li}[\text{PhC}(\text{NAr})_2]$ and FeCl_2 in THF forms the pale yellow ferrate complex $[\{\text{PhC}(\text{NAr})_2\}\text{FeCl}(\mu\text{-Cl})\text{Li}(\text{THF})_3]$ (**1**) (Scheme 1).



Scheme 1

Isolation was performed by extraction with pentane and crystallisation from THF–hexanes. The isolated yields (20–70%) were found to depend critically on the workup conditions. The extraction must be conducted rapidly and at low temperatures as the monoamidinate complex is unstable in hydrocarbon solvents (*vide infra*).

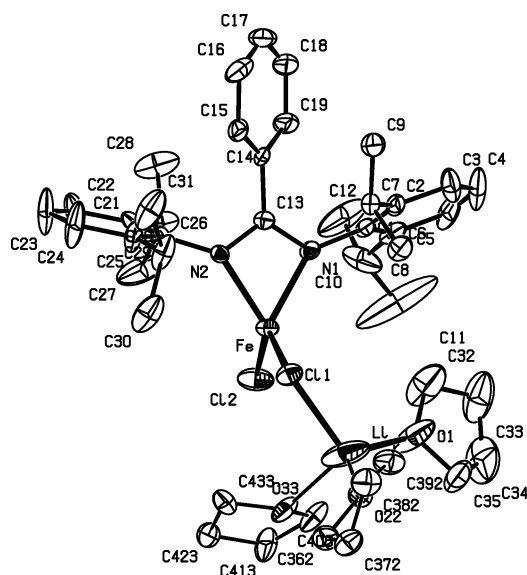
The molecular structure of **1** (Fig. 1) was established by X-ray diffraction. Selected interatomic distances and bond angles are given in Table 1. The asymmetric unit contains one ferrate complex and an uncoordinated THF molecule, which is readily lost from the lattice *in vacuo* or upon drying in a nitrogen stream. The iron centre is pseudotetrahedrally coordinated by a chelating amidinate ligand and two chlorides. One of the chlorides bridges to a lithium ion, which is solvated by three THF molecules. Two of these are heavily disordered (see Experimental for details).

In contrast to the related β -diketiminate ferrate $[\{\text{H}(\text{C}(\text{Me})\text{NAr})_2\}\text{Fe}(\mu\text{-Cl})_2\text{Li}(\text{THF})_2]$,¹³ in which both chlorides bridge the Fe and Li centres, the amidinate complex **1** displays one bridging and one terminal chloride. Consistently, the Cl–Fe–Cl angle in **1** is *ca.* 22° wider than in the β -diketiminate complex,

Dutch Polymer Institute/Center for Catalytic Olefin Polymerization, Stratingh Institute for Chemistry and Chemical Engineering, University of Groningen, Nijenborgh 4, 9747, AG Groningen, The Netherlands
E-mail: b.hessen@rug.nl; Fax: +31 50 363 4315; Tel: +31 50 363 4322

Table 1 Selected bond angles and distances for **1**

Bond lengths/Å			
Fe–C11	2.2778(12)	Fe–N2	2.093(3)
Fe–C12	2.2443(13)	N1–C13	1.327(6)
Fe–N1	2.088(4)	N2–C13	1.337(5)
Bond angles/°			
C11–Fe–C12	118.46(5)	Fe–N1–C1	141.3(3)
C11–Fe–N1	114.46(10)	Fe–N1–C13	92.4(3)
C11–Fe–N2	111.60(8)	C1–N1–C13	124.6(4)
C12–Fe–N1	114.94(10)	Fe–N2–C13	91.9(2)
C12–Fe–N2	121.86(9)	Fe–N2–C20	139.3(2)
N1–Fe–N2	63.76(14)	C13–N2–C20	125.3(3)

**Fig. 1** Molecular structure of **1**. Hydrogen atoms and uncoordinated THF molecule have been omitted for clarity. Thermal ellipsoids at 50%.

in response to the smaller bite angle of the amidinate ligand compared to the β -diketiminato. The aryl rings make angles of 69.4(2) and 80.3(2)° with the N–Fe–N coordination plane. In comparison with the β -diketiminato ferrate complex mentioned above, the aryl groups in **1** are less efficiently shielding the iron centre, as evidenced by the comparatively large C_{ipso} –N–Fe angles (140.3° (av.) for **1** vs. 117.1° (av.) for the β -diketiminato).¹³ The Fe–N distances are identical within experimental error, indicating symmetric coordination of the ligand. The N1–Fe–N2 bite angle (63.78(11)°) is within the range usually observed for amidinates.^{14,15} Delocalisation within the amidinate NCN frame is evidenced by the equal CN bond lengths, although the nitrogen atoms show some slight deviation from planarity ($\Sigma_{N1} = 358.3^\circ$, $\Sigma_{N2} = 356.5^\circ$).

Compound **1** possesses a room temperature magnetic moment $\mu_{\text{eff}} = 5.4 \mu_B$ in benzene, consistent with 4 unpaired electrons in combination with a small orbital contribution.¹⁶ The paramagnetism of **1** is also evident from its ¹H NMR spectrum in C₆D₆. Seven broad resonances are observed between +30 and –30 ppm in a 300 ppm frequency window. The broadness and consequent low intensity of some of the resonances renders integration inaccurate, complicating full interpretation of the spectrum. Nevertheless,

some tentative assignments could be made for the larger signals. For instance, the diastereotopic methyls of the isopropyl groups appear at $\delta - 17.9$ ($\Delta\nu_{1/2} = 356$ Hz, 12H) and $\delta 8.9$ ppm ($\Delta\nu_{1/2} = 169$ Hz, 12H). The presence of only two *i*Pr Me resonances suggests the presence of an exchange process leading to apparent C_{2v} symmetry. Upon dissolution of **1** in THF-*d*₈, a significantly different spectrum is obtained (in addition to the appearance of resonances for free THF, due to exchange of THF coordinated to the Li ion in **1** by THF-*d*₈), suggesting involvement of the solvent. The spectrum displays nine lines with smaller widths compared to solutions in C₆D₆, thus facilitating assignment of the spectrum. Again, the presence of only two signals for the *i*Pr–Me protons and only one *m*-H_{Ar} resonance, suggests a C_{2v} symmetric molecule in solution. It appears that the Lewis basic solvent is able to (reversibly) displace the LiCl moiety to generate the adduct $[\{\text{PhC}(\text{NAr})_2\}\text{FeCl}(\text{THF-}d_8)]$. This is also suggested by the observation that addition of excess pyridine-*d*₅ to C₆D₆ solutions of **1** induces a colour change to deep yellow and formation of a precipitate. Assuming a tetrahedral coordination geometry around Fe, the apparent C_{2v} symmetry can be accounted for by fast site exchange of THF-*d*₈ in the adduct $[\{\text{PhC}(\text{NAr})_2\}\text{FeCl}(\text{THF-}d_8)]$.

The symmetrisation in THF-*d*₈ is fast on the NMR timescale down to –50 °C.

Thermal stability

As noted above, the isolated yield in the preparation of **1** depends strongly on the workup conditions. Solutions of pale yellow **1** in aromatic hydrocarbons or alkane solvents are not stable at room temperature, slowly turning green over the course of several hours with concomitant precipitation of a white solid. The green product was identified by ¹H NMR spectroscopy as the previously described bis(amidinate) complex $[\{\text{PhC}(\text{NAr})_2\}_2\text{Fe}]$ (**2**)¹² (Scheme 1), which could be isolated in 48% yield (based on Fe). The precipitate was not characterised, but mass balance suggests that it consists of LiCl and FeCl₂.

There are several literature examples in which the synthesis of mono(amidinate) transition metal complexes is complicated or thwarted by ligand redistribution leading to bis(amidinate) complexes, regardless of the stoichiometry employed.^{17,18}

Amidinate ligand redistribution can sometimes be circumvented by employing additional chelating donor ligands. Thus, Lee *et al.* isolated the mono(amidinate) complex $[\{\text{PhC}(\text{NAr})(\text{NSiMe}_3)\}\text{FeCl}(\kappa^2\text{-TMEDA})]$ (Ar' = 2,6-Me₂C₆H₃) from reaction of FeCl₂ with the TMEDA adduct of the lithium amidinate at low temperature.¹⁹

A stabilising effect of donor solvents, preventing ligand redistribution, was also observed by Cotton *et al.* in the synthesis of chromium(II) amidinate complexes.²⁰ Accordingly, solutions of **1** in THF-*d*₈ do not show significant formation of the bis(amidinate) complex **2** even after heating at 100 °C for 24 h.

Alkylation

Alkylation of **1** was initially attempted using LiCH(SiMe₃)₂. However, reaction of **1** with the lithium alkyl in THF, followed by pentane extraction, yielded the bis(amidinate) iron complex **2** as the only isolable product. Amidinate scrambling upon alkylation has precedent in the methylation of the Ti(IV)

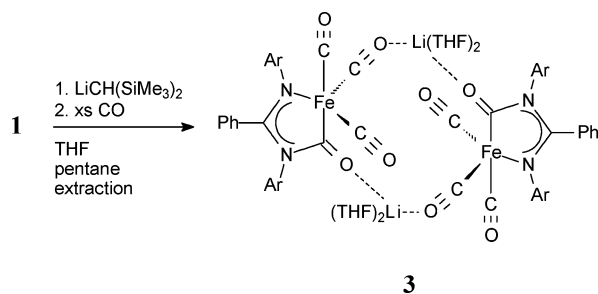
complex $[\{\text{PhC}(\text{NSiMe}_3)_2\}(\mu\text{-Cl})\text{TiCl}_2]_2$. Instead of the desired $[\{\text{PhC}(\text{NSiMe}_3)_2\}\text{TiMe}_3]$, $[\{\text{PhC}(\text{NSiMe}_3)_2\}_2\text{TiMe}_2]$ was isolated, possibly as a result of redistribution of the ligands in the monoamidinate titanium trimethyl complex to give the observed bis(amidinate) species and unstable TiMe_4 .²¹ Similar observations were made by Nelkenbaum *et al.* upon attempted alkylation of Ni(II) monoamidinate complexes.²²

The *in situ* generation of iron alkyl species from **1** was probed by ^1H NMR spectroscopy in $\text{THF-}d_8$. Reactions of **1** with equimolar amounts of KCH_2Ph or $\text{LiCH}_2\text{EMe}_3$ ($\text{E} = \text{C}, \text{Si}$) were accompanied by colour changes from pale yellow *via* red to dark yellow. The ^1H NMR spectra showed formation of new paramagnetic species, presumably the alkyls $[\{\text{PhC}(\text{NAr})_2\}\text{FeR}(\text{THF})]$. The ^1H NMR spectra of these paramagnetic species could not be fully assigned, but some characteristic resonances could be identified by integration (*i*Pr-CH₃, *t*Bu and SiMe₃ groups, see Experimental). In all cases, the ligand *i*Pr-methyl protons show only two resonances (integrating for 12 H each), which suggests fast site exchange of coordinated THF. Pumping off $\text{THF-}d_8$ and redissolution of the residue in cyclohexane- d_{12} again induced amidinate redistribution: the ^1H NMR spectra in this solvent showed mainly the resonances of bis(amidinate) **2**. In an experiment employing $\text{LiCH}_2\text{SiMe}_3$ as the alkylating agent, the alkyl coupling product $\text{Me}_3\text{SiCH}_2\text{CH}_2\text{SiMe}_3$ was detected (GC-MS) in the cyclohexane- d_{12} solution.

Apparently, the putative iron alkyls, like the chloride precursor **1**, decompose in the absence of a donor solvent. The formation of alkyl coupling products suggests that decomposition involves radical pathways, or reductive elimination from FeR_2 species, the latter stemming from the ligand redistribution.

Alkylation in the presence of CO

An attempt was made to trap the putative amidinate iron alkyl species with CO. Earlier it was reported that three-coordinate (β -diketiminate)Fe(alkyl) compounds react with CO to form stable five-coordinate acyl dicarbonyl complexes.²³ Reaction of **1** with $\text{LiCH}(\text{SiMe}_3)_2$ in the presence of excess CO led to the isolation of the dark red dimeric lithium carbamoyl ferrate **3** (Scheme 2).



Scheme 2

Each ferrate anion in **3** contains a formal Fe(0) centre, indicating that a reductive process has taken place. Formation of **3** also involves insertion of carbon monoxide into one of the Fe–N(amidinate) bonds. Hagadorn *et al.* observed insertion of CO into the amidinate complex $[\text{Cp}\{\text{FcC}(\text{NCy})_2\}\text{Fe}(\text{CO})]$ to give the carbamoyl complex $[\text{Cp}\{\text{N}(\text{Cy})\text{C}(\text{Fc})\text{N}(\text{Cy})\text{C}(\text{O})\}\text{Fe}(\text{CO})]$ ($\text{Cy} = \text{c-C}_6\text{H}_{11}$, $\text{Fc} = (\text{C}_5\text{H}_4)\text{Fe}(\text{C}_5\text{H}_5)$).²⁴

Table 2 Selected bond angles and distances for **3**

Bond lengths/Å			
Fe11–N11	1.996(3)	Fe41–N41	1.9961(6)
Fe11–C132	1.927(3)	Fe41–C432	1.935(4)
Fe11–C133	1.769(4)	Fe41–C433	1.766(4)
Fe11–C134	1.798(4)	Fe41–C434	1.798(4)
Fe11–C135	1.725(4)	Fe41–C435	1.720(4)
N11–C113	1.297(4)	N41–C413	1.301(3)
N12–C113	1.384(4)	N42–C413	1.380(3)
N12–C132	1.443(4)	N42–C432	1.443(4)
Bond angles/°			
N11–Fe11–C132	81.01(12)	N41–Fe41–C432	81.05(11)
N11–Fe11–C133	114.80(16)	N41–Fe41–C433	115.63(13)
N11–Fe11–C134	95.13(14)	N41–Fe41–C434	94.72(12)
N11–Fe11–C135	132.59(17)	N41–Fe41–C435	131.53(17)
C132–Fe11–C133	89.19(17)	C432–Fe41–C433	89.21(18)
C132–Fe11–C134	173.36(16)	C432–Fe41–C434	173.01(18)
C132–Fe11–C135	87.90(16)	C432–Fe41–C435	88.49(18)
C133–Fe11–C134	97.36(19)	C433–Fe41–C434	97.66(19)
C133–Fe11–C135	110.93(19)	C433–Fe41–C435	111.4(2)
C134–Fe11–C135	90.81(18)	C434–Fe41–C435	90.21(18)
Fe11–N11–C11	123.4(2)	Fe41–N41–C41	123.25(3)
Fe11–N11–C113	116.2(2)	Fe41–N41–C413	115.99(14)
C11–N11–C113	120.2(3)	C41–N41–C413	120.31(14)
C113–N12–C120	121.8(3)	C413–N42–C420	121.03(18)
C113–N12–C132	115.1(3)	C413–N42–C432	115.2(2)
C120–N12–C132	118.5(2)	C420–N42–C432	119.65(19)
Fe11–C132–O11	132.9(3)	Fe41–C432–O41	132.9(3)
Fe11–C132–N12	112.6(2)	Fe41–C432–N42	112.4(2)
O11–C132–N12	114.4(3)	O41–C432–N42	114.6(3)
N11–C113–N12	115.1(3)	N41–C413–N42	115.3(2)
N11–C113–C114	126.4(3)	N41–C413–C414	125.9(3)
N12–C113–C114	118.3(3)	N42–C413–C414	118.6(3)

The nature of **3** was established by single crystal X-ray diffraction (Fig. 2). Pertinent bond lengths and bond angles are listed in Table 2.

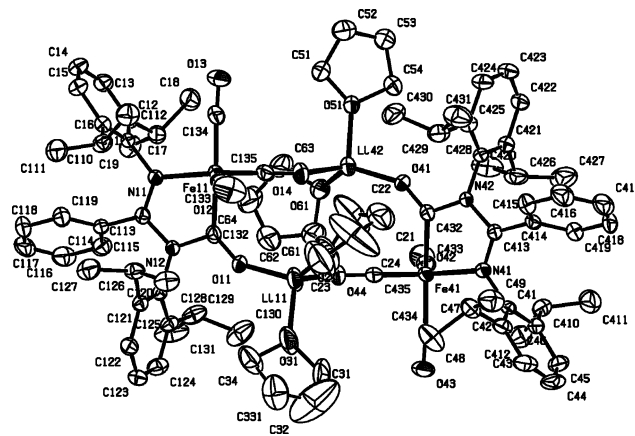


Fig. 2 Molecular structure of **3**. Hydrogen atoms and the uncoordinated THF molecule have been omitted for clarity. Thermal ellipsoids at 50%.

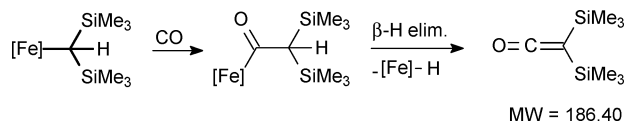
The unit cell contains one diiron compound with a non-crystallographic inversion centre and two non-coordinated THF molecules. The dimer consists of 18 VE $[\{\text{C}(\text{O})\text{N}(\text{Ar})\text{-C}(\text{Ph})\text{N}(\text{Ar})\}\text{Fe}(\text{CO})_3]^-$ ferrate anions bridged by two solvated Li^+ ions. Each iron is bound to a chelating carbamoyl ligand and three carbonyls, one of which is bridging in a linear fashion to the

Li⁺ ion. The latter is also bound to the carbamoyl oxygen of the other ferrate fragment, and two THF molecules.

The ligands establish a distorted trigonal bipyramidal coordination geometry around iron with the carbamoyl carbon and one terminal carbonyl occupying the apical positions (C132–Fe–C134 = 173.36(16)°). The equatorial plane is defined by the carbamoyl nitrogen (N11) and the two other carbonyls, the sum of their angles with the iron centre being 358°. Within the carbamoyl moiety, C113–N11 (1.297(4) Å) is significantly shorter than C113–N12 (1.383(4) Å), giving the former slightly more double bond character. The chelate ring, however, is essentially planar, indicating at least some delocalisation. The linear bridging mode is unusual for the CO ligand, though not unprecedented. In cases where CO acts as a linearly bridging ligand, the most electropositive metal centre is usually bound to the oxygen atom.^{25–27}

Characterisation of **3** by ¹H NMR spectroscopy was frustrated by the persistent presence of metallic iron in the red THF-*d*₈ solutions of this compound, possibly as a result of photolysis of the product. The spectra show broad, overlapping resonances between +10 and 0 ppm. The chemical shift range confirms the diamagnetic nature of **3** as suggested by its 18-valence electron count. The IR spectrum is more informative and consistent with the solid state structure. Absorptions for the terminal carbonyls ($\nu_{\text{CO(term.)}}$) are found at 1883 and 1961 cm^{−1}, while the linearly bridging COs absorb at a lower frequency ($\nu_{\mu\text{-CO}}$ = 1814 cm^{−1}). The carbamoyl CO stretching absorption $\nu_{\text{C(O)N}}$ for **3** is observed at 1556 cm^{−1}. Due to its light-sensitivity and loss of cocrystallised THF from the lattice, no satisfactory elemental analysis could be obtained for the compound.

Although mechanistic details for the formation of **3** are unclear, reduction of Fe(II) is likely to be induced by the alkyl lithium reagent, as ferrate **1** itself does not react with CO under similar conditions. GC-MS analysis of the reaction mixture revealed the presence of bis(trimethylsilyl)methane, probably formed through hydrogen abstraction from the solvent by bis(trimethylsilyl)methyl radicals. The coupling product of CH(SiMe₃)₂ radicals, 1,1,2,2-tetrakis(trimethylsilyl)ethane, however, was not observed, suggesting that reductive elimination from a dialkyliron(II) species does not take place here. The chromatogram also showed the presence of a compound with *m/z* = 186, which corresponds to bis(trimethylsilyl)ketene (Me₃Si)₂C=C=O.²⁸ The ketene might be the β-H-elimination product of an iron acyl complex [Fe]–C(O)CH(SiMe₃)₂, which in turn could be formed by CO insertion into the Fe–C bond of an iron alkyl species (Scheme 3).



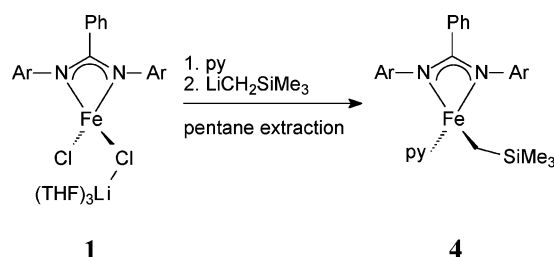
Scheme 3 Possible mechanism for the formation of bis(trimethylsilyl)ketene.

Alkylation in the presence of pyridine

The NMR tube scale alkylation experiments described above suggest that substitution of chloride in **1** for an alkyl ligand is

possible, but that a Lewis base is required to suppress ligand redistribution leading to **2**.

Apparently, THF is an insufficiently strong base to remain bound to iron during the workup procedure. Therefore, alkylation of **1** was studied in the presence of a stronger donor ligand than THF. In a one-pot reaction, ferrate **1** was generated in THF and reacted *in situ* with pyridine followed by addition of LiCH₂SiMe₃. Extraction with pentane and crystallisation from the same solvent afforded orange crystals of [{PhC(NAr)₂}FeCH₂SiMe₃(py)] (**4**) in 38% isolated yield (Scheme 4). The modest isolated yield appears to be mainly due to the high solubility of **4** in pentane.



Scheme 4

Fig. 3 shows the solid state structure of **4** as determined by X-ray diffraction. The asymmetric unit contains two independent molecules of the iron complex. In view of their structural similarity, only one of these is discussed here. Pertinent bond lengths and bond angles for **4** are listed in Table 3.

The iron centre in **4** is ligated in a distorted tetrahedral fashion with angles between the coordinating atoms in the range of 64–135°. The bite angle (N11–Fe–N12 = 63.62(7)°) is close to that in **1**. The amidinate ligand is bound to Fe in the chelating mode, although slightly less symmetrically than in **1**, as evidenced by small, but significant differences in the Fe–N and amidinate C–N distances ($\Delta_{\text{Fe-N}} \approx 0.04$ Å, $\Delta_{\text{C-N}} \approx 0.03$ Å). This small tendency towards amido-imino character is also evident from the full planarity of N12 ($\Sigma_{\text{LN12}} = 359.65^\circ$), while N11 is more distorted ($\Sigma_{\text{LN11}} = 354.80^\circ$). The pyridine ligand is roughly orthogonal (84.58(11)°) to the Fe–N–C–N coordination plane, while the aryl groups and the phenyl ring are inclined at 66.15(10), 74.83(10) (Ar) and 43.42(10)° (Ph) with respect to this plane. The Fe–C distance in **4** (2.049(2) Å) is similar to

Table 3 Selected bond angles and distances for **4**

Bond lengths/Å			
Fe1–N11	2.0864(18)	Fe1–C137	2.049(2)
Fe1–N12	2.1226(18)	N11–C113	1.351(3)
Fe1–N13	2.1314(18)	N12–C113	1.323(3)
Bond angles/°			
N11–Fe1–N12	63.62(7)	Fe1–N12–C113	91.67(13)
N11–Fe1–N13	107.47(7)	Fe1–N12–C120	141.52(14)
N12–Fe1–N13	101.65(7)	C113–N12–C120	126.46(18)
C137–Fe1–N11	135.02(8)	Fe1–N13–C132	118.43(15)
C137–Fe1–N12	122.06(9)	Fe1–N13–C136	124.14(15)
C137–Fe1–N13	113.63(9)	C132–N13–C136	117.02(19)
Fe1–N11–C11	140.06(13)	N11–C113–N12	112.14(18)
Fe1–N11–C113	92.43(13)	N11–C113–C114	122.25(19)
C11–N11–C113	122.31(18)	N12–C113–C114	125.52(19)
		Fe1–C137–Si1	118.76(14)

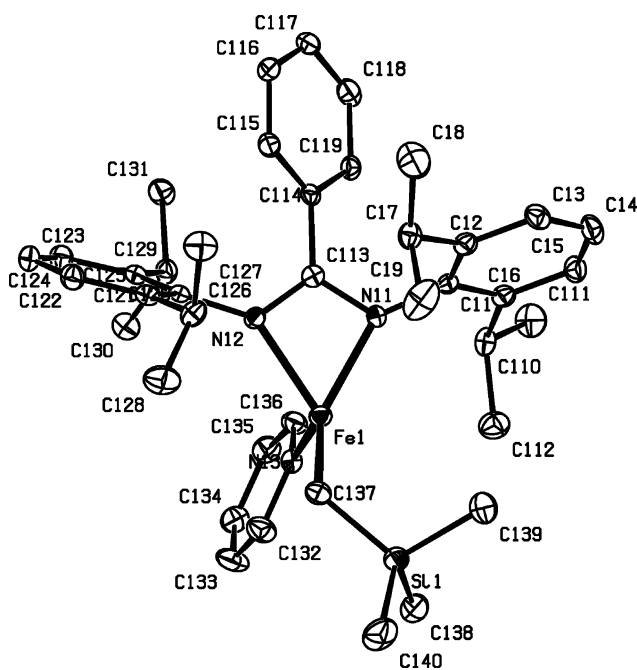


Fig. 3 X-Ray structure of **4**. Hydrogen atoms have been omitted for clarity. Thermal ellipsoids at 50%.

those observed in the four-coordinate bis(trimethylsilylmethyl) compounds $[(\text{NN})\text{Fe}(\text{CH}_2\text{SiMe}_3)_2]$ (NN = chelating diamine or diimine, $\text{Fe}-\text{C} = 2.042(3)-2.0963(13)$ Å) reported by Bart *et al.*²⁹

The $\text{Fe}-\text{C}-\text{Si}$ angle ($118.76(14)^\circ$) is relatively large, probably in response to steric interactions between the trimethylsilyl group and the *i*Pr substituents of the ligand. Steric crowding is also evident from the unsymmetric $\text{C}-\text{Fe}-\text{N}$ (amidinate) angles of $135.02(8)$ and $122.06(9)^\circ$.

Monoalkyl complex **4** has an effective magnetic moment $\mu_{\text{eff}} = 5.5 \mu_{\text{B}}$ in benzene at ambient temperature. The high-spin nature of the compound is also manifested in the ^1H NMR spectrum which consists of broad and shifted lines. The spectrum indicates an averaged C_{2v} symmetry in solution as judged from the presence of only two *i*Pr–Me resonances (δ 5.0 and -25.0 ppm, 12 H each) and one *m*- H_{Ar} resonance (δ 11.6 ppm, 4H). The apparent C_{2v} symmetry of the molecule can be accounted for by fast site exchange of the pyridine molecule on the NMR timescale. The related four-coordinate pyridine adduct $[\{\text{HC}(\text{C}(\text{Me})\text{NAr})_2\}\text{FeCH}_2\text{Ph}(\text{py})]$ of the β -diketiminate monobenzyl complex was found to exhibit similar site exchange of the pyridine ligand.³⁰ Taking the fluxional process into account, the number of observed resonances (9) is smaller than expected (13), leaving 4 resonances unobserved. This could be due to extreme line broadening for protons close to the paramagnetic centre (*e.g.* *o*- H_{py} , $\text{Fe}-\text{CH}_2$, *o*- H_{Ph} , *i*Pr–CH). The SiMe_3 proton resonances of the alkyl ligand (9H) are found at δ 35.6 ppm. The assignments of the 5 remaining peaks are ambiguous due to their similar integrals (1H or 2H).

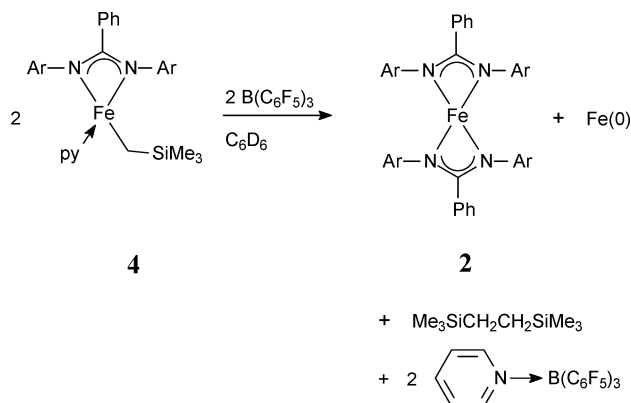
Reactivity with Lewis acids and ethene

Using methyl alumoxane (MAO) as cocatalyst ($\text{Al}/\text{Fe} = 500$), the chloride complex **1** and alkyl derivative **4** were tested for activity in ethene polymerisation ($P_{\text{C}_2\text{H}_4} = 10$ bar, $T = 50^\circ\text{C}$). In neither case was significant ethene consumption seen, and no polymer

was obtained. The observed lack of activity for **4**/MAO contrasts with the patent literature, in which the benzamidinate iron alkyl complex $[\{\text{PhC}(\text{N}-2,4,6-\text{Me}_3\text{C}_6\text{H}_2)_2\}\text{FeCH}_2\text{SiMe}_3(\text{py})]$ is claimed as a catalyst precursor for olefin polymerisation upon activation with aluminoxanes or $\text{B}(\text{C}_6\text{F}_5)_3$ (although characterisation data or activity figures are not provided for this specific iron complex).³¹

The reaction of **4** with the Lewis acid $\text{B}(\text{C}_6\text{F}_5)_3$ could proceed either by alkyl abstraction, or by abstraction of the pyridine base. The latter reaction is seen to occur upon treatment **4** with $\text{B}(\text{C}_6\text{F}_5)_3$ in C_6D_6 . The major products, as detected by ^1H and ^{19}F NMR spectroscopy, are the pyridine adduct of the borane (identified by independent generation from $\text{B}(\text{C}_6\text{F}_5)_3$ and pyridine in C_6D_6) and the bis(amidinate) complex $[\{\text{PhC}(\text{NAr})_2\}_2\text{Fe}]$ (**2**). A black film was deposited on the walls of the NMR tube suggesting coformation of $\text{Fe}(0)$. Consistently, 1,2-bis(trimethylsilyl)ethane was detected by GC-MS analysis.

These products can be accounted for by the stoichiometry shown in Scheme 5. Formation of **2** upon pyridine abstraction from **4** is consistent with the instability of three-coordinate $\text{Fe}(\text{II})$ complexes of $[\text{PhC}(\text{NAr})_2]^-$ described above.



Scheme 5

Conclusions

Mono(amidinate) iron(II) complexes with the sterically demanding amidinate $[\text{PhC}(\text{NAr})_2]^-$ ($\text{Ar} = 2,6\text{-}i\text{Pr}_2\text{C}_6\text{H}_3$) can be prepared, but are subject to ligand redistribution processes in the absence of additional Lewis bases. In contrast to the corresponding β -diketiminate ligand, the orientation of the 2,6-*i*Pr₂C₆H₃ substituents in the amidinate apparently offers insufficient steric protection to stabilise three-coordinated alkyl complexes of the type $[\{\text{PhC}(\text{NAr})_2\}\text{FeR}]$. Nevertheless, four-coordinated (mono)amidinate $\text{Fe}(\text{II})$ alkyls can be generated as their Lewis-base adducts $[\{\text{PhC}(\text{NAr})_2\}\text{FeR}(\text{L})]$, although THF is too weakly coordinating to allow the isolation of these compounds. This is possible when the stronger base pyridine is used.

Experimental

General considerations

All complexes are air-sensitive and were handled under a dry dinitrogen atmosphere using standard Schlenk and drybox techniques. THF (99.9% Aldrich) was percolated over a column

of Al₂O₃ and stored under nitrogen. Hexane and pentane (99.9% Aldrich) were percolated over a column packed with molecular sieves 4 Å (90 wt%) and Al₂O₃ (10 wt%) and stored under nitrogen. Toluene (99.9% Aldrich) used for polymerisation experiments was percolated over a column packed with molecular sieves 4 Å (90 wt%) and Al₂O₃ (10 wt%) and freed of oxygen by passing it over BASF-R3-11 supported Cu-catalyst. Pyridine was dried over CaH₂. Deuterated solvents (Aldrich) were dried over Na/K alloy (C₆D₆, THF-*d*₈, cyclohexane-*d*₁₂) or used as received and stored under nitrogen.

Instrumentation

NMR spectra were recorded on Varian Inova 500, VXR 300 and Varian Gemini 200 MHz instruments. ¹H NMR chemical shifts are reported in ppm relative to residual protiated solvent in C₆D₆ (7.15 ppm) or THF-*d*₈ (3.57 ppm). Shifts for paramagnetic compounds are followed by their linewidth at half height (in Hz), integrals, and assignment where possible. IR spectra were recorded on a Mattson 4020 Galaxy FT-IR spectrometer. GC-MS analyses were conducted using a HP 5973 mass-selective detector attached to a HP 6890 GC instrument. Elemental analyses were performed by the Microanalytical Department at the University of Groningen or by Mikroanalytisches Laboratorium H. Kolbe, Mülheim an der Ruhr, Germany. Reported values are the averages of two independent determinations. Solution effective magnetic moments were determined at 298 K in C₆H₆/C₆D₆ (0.375 mL/0.125 mL) according to Evans' method.³² Magnetic data were corrected for diamagnetism using Pascal's constants.³³ Effective magnetic moments were calculated as $\mu_{\text{eff}} = 2.828 \sqrt{\chi_m T}$.

X-Ray structure determinations

Collection, refinement and crystallographic data are given in Table 4.

1. Suitable crystals were obtained by slow cooling of a hexane–THF solution to –30 °C. The crystal was picked from the mother liquor and was covered with inert oil to avoid deterioration due to loss of solvent from the crystal lattice. Some atoms (C24, C32, C64) belonging to the coordinated THF molecules showed unrealistic displacement parameters when allowed to vary anisotropically, suggesting dynamic disorder. The most heavily disordered THF ligands (ring 2 : O2–C36.C39 and ring 3 : O3–C40.C43) have been described by two site occupancy factors each. The s.o.f.s of the major fractions refined to values of 0.533(6) and 0.518(6), respectively.

3. Suitable crystals were obtained by recrystallisation from THF. The electron density of C33 was disordered over two positions, indicating conformational disorder. The s.o.f. of the major fraction of the component of the twin model refined to a value of 0.70(1). Some other atoms (O31, C31, C32, C64) belonging to the coordinated THF molecules also showed unrealistic displacement parameters suggesting some degree of disorder, which is in line with the weak scattering power of the crystals investigated.

4. Suitable crystals were obtained by recrystallisation from pentane. Some atoms (C230 and C231) showed unrealistic displacement parameters when allowed to vary anisotropically, suggesting dynamic disorder. The smeared electron density for

C230 and C231 has been described by two site occupancy factors with separately refined displacement parameters. The s.o.f. of the major fraction of the component of the disorder model refined to a value of 0.612(10).

CCDC reference numbers 610249–610251. For crystallographic data in CIF or other electronic format see DOI: 10.1039/b608108h

Starting materials and reagents

Anhydrous FeCl₂,³⁴ FeCl₂(THF)_{1.5},³⁵ LiCH₂SiMe₃,³⁶ LiCH₂–CMe₃,³⁷ LiCH(SiMe₃)₂,³⁸ KCH₂Ph³⁹ and B(C₆F₅)₃⁴⁰ were prepared according to literature procedures. [N,N'-bis(2,6-diisopropylphenyl)benzamidinium]⁴¹ was deprotonated by standard methodology using *n*BuLi (2.5 M in hexanes) in THF at RT.¹²

All other chemicals are commercially available and were used without further purification.

Preparation of [{PhC(NAr)₂}FeCl₂Li(THF)₃].THF (1)

A solution of Li[PhC(NAr)₂] (1.02 g, 2.27 mmol) in THF (15 mL) was added to a suspension of FeCl₂ (0.287 g, 2.27 mmol) in THF (10 mL) at 0 °C and the reaction mixture was stirred for 1 h at 0 °C. The solvent was removed *in vacuo* and residual THF was removed by stirring the mixture with pentane (10 mL) which was subsequently removed *in vacuo*. The product was extracted at 0 °C with pentane (40 mL) until the pentane was colourless. The combined extracts were evaporated to dryness, leaving a yellow solid. The solid was washed with cold pentane (15 mL, 2 times). The crude product was recrystallised from THF–hexane at –30 °C, yielding yellow crystals. Yield: 1.22 g (1.59 mmol, 70%).

μ_{eff} (C₆H₆, 298 K) = 5.4 μ_{B} .

¹H NMR (300 MHz, C₆D₆, RT): δ ($\Delta\nu_{1/2}$) = 23.1 (73 Hz, 2H), 18.7 (800 Hz), 13.2 (415 Hz), 8.9 (169 Hz, 12H, *i*Pr–CH₃), 6.3 (90 Hz, 12H, coord. THF), 2.7 (65 Hz, 12H, coord. THF), –17.9 (356 Hz, 12H, *i*Pr–CH₃) ppm (Hz).

¹H NMR (500 MHz, THF-*d*₈, RT): δ ($\Delta\nu_{1/2}$) = 19.0 (23 Hz, 2H, *m*-H_{Ph}), 15.6 (32 Hz, 4H, *m*-H_{Ar}), 14.6 (849 Hz, 4H, *i*Pr–CH), 11.8 (134 Hz, 2H, *o*-H_{Ph}), 5.5 (45 Hz, 12H, *i*Pr–CH₃), 3.6 (16 Hz, 12H, THF), 2.3 (20 Hz, 1H, *p*-H_{Ph}), 1.7 (13 Hz, 12H, THF), –12.9 (171 Hz, 12H, *i*Pr–CH₃), –22.5 (24 Hz, 2H, *p*-H_{Ar}) ppm.

IR (nujol mull, KBr): ν_{max} /cm^{–1} 1623w, 1580m, 1326s, 1272s, 1253s, 1238s, 1183w, 1097w, 1045s, 959m, 935w, 919w, 893 m, 803w, 784m, 766s, 696s.

Anal. Found: C, 64.89; H, 8.04; N, 3.57; Fe, 6.98; Li, 0.84. Calc. for C₄₃H₆₃Cl₂FeLiN₂O₃: C, 65.40; H, 8.04; N, 3.55; Fe, 7.07; Li, 0.88%.

Thermally induced ligand rearrangement of 1

A suspension of **1** (0.30 g, 0.38 mmol) in pentane (40 mL) was stirred at room temperature for 48 h. During this period, the colour changed from yellow to dark green and precipitation of a white salt was observed. The solution was filtered and concentration of the filtrate to *ca.* 5 mL afforded **2** as a dark green crystals. Yield 0.17 g (0.18 mmol, 48% based on Fe). The spectroscopic (IR, ¹H NMR) properties of the product correspond to those reported previously for **2**.¹²

Table 4 Collection and crystallographic data for **1**, **3** and **4**

	1	3	4
Formula	C ₄₃ H ₆₃ N ₂ O ₃ FeCl ₂ Li·THF	C ₈₆ H ₁₁₀ N ₄ O ₁₂ Fe ₂ ·2THF	C ₄₀ H ₅₅ N ₃ FeSi
FW	861.78	1661.63	661.82
Cryst. dim./mm	0.22 × 0.21 × 0.20	0.35 × 0.27 × 0.15	0.50 × 0.34 × 0.24
Colour, habit	Yellow, block	Red, irregular	Orange, prism
Crystal system	Triclinic	Monoclinic	Monoclinic
Space group, no. ⁴²	<i>P</i> $\bar{1}$, 2	<i>P</i> 2 ₁ / <i>c</i> , 14	<i>P</i> 2 ₁ / <i>c</i> , 14
<i>a</i> /Å	13.1932(7)	21.5290(1)	22.329(1)
<i>b</i> /Å	13.4944(7)	10.7289(5)	17.831(1)
<i>c</i> /Å	14.321(1)	39.956(2)	20.489(1)
<i>a</i> /°	79.239(1)	90	90
<i>β</i> /°	84.262(1)	91.712(1)	109.342(1)
<i>γ</i> /°	72.039(1)	90	90
<i>Z</i>	2	4	4
<i>V</i> /Å ³	2380.3(2)	8994.1(8)	7697.2(7)
<i>ρ</i> _{calc} /g cm ^{−3}	1.202	1.227	1.142
<i>θ</i> range/°	2.23–20.34	2.17–24.43	2.25–26.72
<i>λ</i> /Å	0.71073 (Mo Kα)	0.71073 (Mo Kα)	0.71073 (Mo Kα)
<i>T</i> /K	100(1)	110(1)	100(1)
Data collect. time/h	7.9	13.0	8.0
No. of meas. refl.	22682	63345	60961
No. of unique refl.	11506	15868	15636
<i>R</i> _{int}	0.0841	0.0530	0.0609
<i>μ</i> /cm ^{−1}	4.71	3.86	4.52
No. of parameters	634	1041	1250
Weighting scheme: <i>a</i> , <i>b</i> ^a	0.0514, 0.0	0.0795, 15.4628	0.0509, 0.0148
<i>R</i> (<i>F</i>) for <i>F</i> _o ≥ 4σ(<i>F</i> _o) ^b	0.0728	0.0683	0.0440
w <i>R</i> (<i>F</i> ²) ^c	0.1628	0.1841	0.1057
Res. el. dens./e Å ^{−3}	−0.44, 0.58(8)	−0.75, 0.86(7)	−0.25, 0.46(6)
GoF ^d	0.984	1.027	1.018

^a $w = 1/[\sigma^2(F_o^2) + (aP)^2 + bP]$, $P = [\max(F_o^2, 0) + 2F_c^2]/3$, ^b $R(F) = \Sigma(|F_o| - |F_c|)/\Sigma |F_o|$, ^c $wR(F^2) = [\Sigma[w(F_o^2 - F_c^2)^2]/\Sigma[w(F_o^2)^2]]^{1/2}$, ^d $GoF = [\Sigma[w(F_o^2 - F_c^2)^2]/(n - p)]^{1/2}$, *n* = # refl., *p* = # param. refined.

Reaction of **1** with LiCH₂SiMe₃

LiCH₂SiMe₃ (3.6 mg, 38 μmol) was added to a solution of **1** (30 mg, 38 μmol) in THF-*d*₈ (0.5 mL). A colour change from pale yellow *via* red to dark yellow was observed. ¹H NMR data for the new species:

¹H NMR (500 MHz, THF-*d*₈, RT): δ (Δ*v*_{1/2}) = 19.3 (44 Hz, 1H), 16.9 (254 Hz, 9H, SiMe₃), 13.4 (109 Hz, 4H), 10.5 (166 Hz, 1H), 6.8 (40 Hz, 5H), 6.6 (48 Hz, 2H), 5.5 (480 Hz, 12H, *i*Pr-CH₃), 3.6 (29 Hz, 16H, THF), 1.72 (24 Hz, 16H, THF), −12.4 (302 Hz, 12H, *i*Pr-CH₃), −21.5 (45 Hz, 1H) ppm.

Reaction of **1** with LiCH₂CMe₃

LiCH₂CMe₃ (3.0 mg, 38 μmol) was added to a solution of **1** (30 mg, 38 μmol) in THF-*d*₈ (0.5 mL). A colour change from pale yellow *via* red to dark yellow was observed. ¹H NMR data for the new species:

¹H NMR (500 MHz, THF-*d*₈, RT): δ (Δ*v*_{1/2}) = 43.0 (490 Hz, 9H, *t*Bu), 20.7 (27 Hz, 2H), 14.4 (247 Hz, 2H), 13.0 (232 Hz, 4H), 5.5 (66 Hz, 12H, *i*Pr-CH₃), 3.6 (13 Hz, 12H, THF), 1.7 (13 Hz, 12H, THF), −12.7 (194 Hz, 2H), −14.9 (348 Hz, 12H, *i*Pr-CH₃), −21.3 (25 Hz, 2H) ppm.

Reaction of **1** with KCH₂Ph

KCH₂Ph (5.0 mg, 38 μmol) was added to a solution of **1** (30 mg, 38 μmol) in THF-*d*₈ (0.5 mL). A colour change from pale yellow

via red to dark yellow was observed. Precipitation of KCl was noted. ¹H NMR data for the new species:

¹H NMR (500 MHz, THF-*d*₈, RT): δ (Δ*v*_{1/2}) = 55.9 (1599 Hz), 35.5 (143 Hz), 31.8 (193 Hz), 29.9 (213 Hz), 21.9 (233 Hz), 20.5 (122 Hz), 19.4 (257 Hz), 16.9 (206 Hz), 15.7 (197 Hz), 14.7 (363 Hz), 13.9 (166 Hz), 12.4 (337 Hz), 5.4 (421 Hz), 3.6 (55 Hz, THF), 1.7 (53 Hz, THF), −1.7 (441 Hz), −5.4 (212 Hz), −6.3 (798 Hz), −11.0 (470 Hz), −13.2 (1317 Hz), −14.3 (264 Hz), −18.7 (994 Hz), −19.7 (269 Hz), −21.1 (114 Hz), −29.3 (667 Hz), −44.5 (539 Hz), −55.9 (126 Hz) ppm.

Preparation of [{C(O)(2,6-*i*Pr₂C₆H₃)NC(Ph)N(2,6-*i*Pr₂C₆H₃)}-Fe(CO)₂-μ-((CO)Li(THF)₂)₂·2THF (**3**)

All manipulations were performed at 0 °C. A solution of Li[PhC(NAr)₂] (1.02 g, 2.27 mmol) in THF (10 mL) was added to a suspension of FeCl₂ (0.144 g, 1.13 mmol) in THF (5 mL) and the reaction mixture was stirred for 1 hour. A solution of LiCH(SiMe₃)₂ (0.188 g, 1.13 mmol) in THF (10 mL) was added dropwise to the reaction mixture in 30 min. After 30 min the reaction mixture was degassed and CO was admitted. After 3 h, the solution was allowed to warm to RT and THF was removed *in vacuo*. The residue was extracted with pentane (30 mL, 3×) and hot hexane (30 mL, 1×). The alkane solvent was removed *in vacuo* and the crude product was dissolved in THF. The solution was concentrated and pentane was slowly diffused into the solution yielding dark red, block-shaped crystals (0.20 g, 0.12 mmol, 21% based on FeCl₂).

IR (nujol mull, KBr): $\nu_{\text{max}}/\text{cm}^{-1}$ 3058w, 1961s (C≡O), 1883s (C≡O), 1814s (C≡OLi), 1582w, 1556s (C=O), 1526w, 1493w, 1320w, 1262w, 1175w, 1103w, 1054m, 1009m, 913w, 834w, 805w, 784w, 747w, 711m, 696w, 679w, 631w, 587w, 551w, 538w, 477w.

^1H NMR analysis of the complex was frustrated by the formation of Fe(0) in the NMR tube, possibly due to photolysis. Broad, overlapping signals were observed in the diamagnetic region (+10–0 ppm).

Satisfactory elemental analysis for **3** could not be obtained due to the light-sensitivity of the crystals and the fact that cocrystallised THF is easily lost from the lattice.

Preparation of $[\{\text{PhC}(\text{NAr})_2\}\text{Fe}(\text{CH}_2\text{SiMe}_3)(\text{py})]$ (**4**)

N,N'-2,6-(Diisopropylphenyl)benzamidine (780 mg, 1.77 mmol) was dissolved in THF (20 mL). *n*-BuLi (2.5 M in hexanes, 0.7 mL, 1.77 mmol) was added. The darkened solution was stirred for 30 min and transferred to a dropping funnel. The Li-amidinate solution was added dropwise to a stirred suspension of $\text{FeCl}_2(\text{THF})_{1.5}$ (416 mg, 1.77 mmol) in THF (10 mL). After 1 h, pyridine (0.3 mL, 3.7 mmol) was added to the dark yellow solution. The colour of the solution became more intensely yellow in the course of 15 min. $\text{LiCH}_2\text{SiMe}_3$ (167 mg, 1.77 mmol) was added, resulting in a dark yellow solution. After stirring for 15 min, all volatiles were pumped off. Residual THF/excess pyridine were removed by suspending the residue in hexanes and subsequent removal of all volatiles *in vacuo* (10 mL, 4×). The residue was then extracted with hexanes (30 mL, 3×), leaving an off-white salt. Cooling to -25°C afforded orange crystals. Yield 440 mg (0.66 mmol, 38%).

$$\mu_{\text{eff}}(\text{C}_6\text{H}_6, 298\text{ K}) = 5.5\ \mu_{\text{B}}.$$

^1H NMR (500 MHz, C_6D_6 , RT) δ ($\Delta\nu_{1/2}$) = 83.3 (1980 Hz, 2H), 35.6 (200 Hz, 9H, SiCH_3), 31.8 (233 Hz, 2H), 27.5 (195 Hz, 2H), 26.0 (25 Hz, 2H), 11.6 (176 Hz, 4H, *m*- H_{Ar}), 5.0 (752 Hz, 12H, *i*Pr- CH_3), -19.9 (22 Hz, 2H, *p*- H_{Ar}), -25.0 (435 Hz, 12H, *i*Pr- CH_3) ppm.

IR (nujol mull, KBr) $\nu_{\text{max}}/\text{cm}^{-1}$ = 3053m, 2962s, 2905s, 2893s, 1601w, 1579w, 1507s, 1482s, 1454s, 1434s, 1401s, 1360s, 1316, 1270m, 1251m, 1239s, 1214m, 1177w, 1153w, 1121w, 1098m, 1068w, 1053w, 1042w, 1027w, 1011w, 951w, 935w, 917w, 874, 851m, 824m, 808m, 785m, 770m, 761m, 751m, 738m, 724m, 697s, 551w, 539m, 510m, 492w, 477w cm^{-1} .

Anal. Found: C, 72.83; H, 8.45; N, 6.44. Calc. for $\text{C}_{40}\text{H}_{35}\text{N}_3\text{FeSi}$: C, 72.59; H, 8.38; N, 6.35%.

Reaction of **4** with $\text{B}(\text{C}_6\text{F}_5)_3$

$\text{B}(\text{C}_6\text{F}_5)_3$ (25 mg, 49 μmol) was added to a solution of **4** (30 mg, 49 μmol) in C_6D_6 (0.5 mL). A colour change from bright orange to yellow was observed. By ^1H and ^{19}F NMR spectroscopy, the formation of **2** and $\text{C}_5\text{H}_5\text{NB}(\text{C}_6\text{F}_5)_3$ was observed. 1,2-Bis(trimethylsilyl)ethane was detected by GC-MS analysis.

NMR data for $\text{C}_5\text{H}_5\text{NB}(\text{C}_6\text{F}_5)_3$:

^1H NMR (300 MHz, C_6D_6 , RT): δ = 8.01 (2H, *o*-H), 6.80 (1H, *p*-H), 6.40 (2H, *m*-H) ppm.

^{19}F NMR (188 MHz, C_6D_6 , RT): δ = -131.4 (d, J_{FF} = 19.2 Hz, 2F, *o*-F), -155.2 (t, J_{FF} = 21.1 Hz, 1F, *p*-F), -162.3 (m, 2F, *m*-F) ppm.

Ethene polymerisation tests with **1** and **4**

A stainless steel 1L autoclave (Medimex), fully temperature and pressure controlled and equipped with solvent and catalyst injection systems, was preheated *in vacuo* for 45 min at 100°C prior to use. The reactor was cooled to 50°C , charged with 250 mL of toluene and pressurised with ethene (10 bar). Cocatalyst (PMAO solution in toluene, 4.9 wt% Al (Al/Fe = 500)) was injected, followed by injection of the Fe complex in toluene (20 μmol in 5 mL). Temperature and pressure were monitored. After 30 min the runs were aborted by venting the reactor and addition of ethanol. Excess MAO was further destroyed by treatment of the toluene solution with ethanol/dilute hydrochloric acid. No significant amount of polymer was obtained.

References

- 1 M. W. Bouwkamp, S. C. Bart, E. J. Hawrelak, R. J. Trovitsch, E. Lobkovsky and P. J. Chirik, *Chem. Commun.*, 2005, 3406.
- 2 M. W. Bouwkamp, E. Lobkovsky and P. J. Chirik, *J. Am. Chem. Soc.*, 2005, **27**, 9660.
- 3 (a) G. J. P. Britovsek, V. C. Gibson, B. S. Kimberley, P. J. Maddox, S. J. McTavish, G. A. Solan, A. J. P. White and D. J. Williams, *Chem. Commun.*, 1998, 849; (b) B. L. Small, M. Brookhart and A. M. A. Bennett, *J. Am. Chem. Soc.*, 1998, **120**, 4049.
- 4 S. C. Bart, E. J. Hawrelak, A. K. Schmisser, E. Lobkovsky and P. J. Chirik, *Organometallics*, 2004, **23**, 237.
- 5 A. R. Hermes and G. S. Girolami, *Organometallics*, 1987, **6**, 763.
- 6 J. L. Kisko, T. Hascall and G. Parkin, *J. Am. Chem. Soc.*, 1998, **120**, 10561.
- 7 (a) M. Akita, N. Shirasawa, S. Hikichi and Y. Mora-oka, *Chem. Commun.*, 1998, 973; (b) N. Shirasawa, M. Akita, S. Hikichi and K. Morokuma, *Chem. Commun.*, 1999, 417; (c) N. Shirasawa, T. T. Nguyen, S. Hikichi, Y. Moro-oka and M. Akita, *Organometallics*, 2001, **20**, 3582.
- 8 V. C. Gibson, S. K. Spitzmesser, A. J. P. White and D. J. Williams, *J. Chem. Soc., Dalton Trans.*, 2003, 2718.
- 9 M. D. Fryzuk, D. B. Leznoff, E. S. F. Ma, S. J. Rettig and V. G. Young, Jr., *Organometallics*, 1998, **17**, 2313.
- 10 (a) J. M. Smith, R. J. Lachicotte and P. L. Holland, *Organometallics*, 2002, **21**, 4808; (b) H. Andres, E. L. Bominaar, J. M. Smith, N. A. Eckert, P. L. Holland and E. Münck, *J. Am. Chem. Soc.*, 2002, **124**, 3012; (c) J. Vela, J. M. Smith, R. J. Lachicotte and P. L. Holland, *Chem. Commun.*, 2002, 2886; (d) J. Vela, S. Vaddadi, T. R. Cundari, J. M. Smith, E. A. Gregory, R. J. Lachicotte, C. J. Flaschenriem and P. L. Holland, *Organometallics*, 2004, **23**, 5226.
- 11 T. J. J. Sciarone, A. Meetsma, B. Hessen and J. H. Teuben, *Chem. Commun.*, 2002, 1580.
- 12 C. A. Nijhuis, E. Jellema, T. J. J. Sciarone, A. Meetsma, P. H. M. Budzelaar and B. Hessen, *Eur. J. Inorg. Chem.*, 2005, 2089.
- 13 J. M. Smith, R. J. Lachicotte and P. L. Holland, *Chem. Commun.*, 2001, 1542.
- 14 F. T. Edelmann, *Coord. Chem. Rev.*, 1994, **137**, 403.
- 15 J. Barker and M. Kilner, *Coord. Chem. Rev.*, 1994, **133**, 219.
- 16 A. Earnshaw, *Introduction to Magnetochemistry*, Academic Press Inc. Ltd., London, 1968.
- 17 P. J. Stewart, A. J. Blake and P. Mountford, *Inorg. Chem.*, 1997, **36**, 1982.
- 18 J. A. R. Schmidt and J. Arnold, *J. Chem. Soc., Dalton Trans.*, 2002, 3454.
- 19 H. K. Lee, T. S. Lam, C.-K. Lam, H.-W. Li and S. M. Fung, *New J. Chem.*, 2003, **27**, 1310.
- 20 F. A. Cotton, L. M. Daniels, C. A. Murillo and P. Schooler, *J. Chem. Soc., Dalton Trans.*, 2000, 2001.
- 21 J. C. Flores, J. C. W. Chien and M. D. Rausch, *Organometallics*, 1995, **14**, 1827.
- 22 E. Nelkenbaum, M. Kapon and M. S. Eisen, *Organometallics*, 2005, **24**, 2645.
- 23 J. M. Smith, R. J. Lachicotte and P. L. Holland, *Organometallics*, 2002, **21**, 4808.
- 24 J. R. Hagadorn and J. Arnold, *J. Organomet. Chem.*, 2001, **637–639**, 521.

-
- 25 H. Deng and S. G. Shore, *Inorg. Chem.*, 1992, **31**, 2289.
26 J. A. Marsella, J. C. Huffman, K. G. Caulton, B. Longato and J. R. Norton, *J. Am. Chem. Soc.*, 1982, **104**, 6360.
27 D. M. Hamilton, Jr., W. S. Willis and G. D. Stucky, *J. Am. Chem. Soc.*, 1981, **103**, 4255.
28 B. L. Groh, G. R. Magrum and T. J. Barton, *J. Am. Chem. Soc.*, 1987, **109**, 7568.
29 S. C. Bart, E. J. Hawrelak, A. K. Schmisser, E. Lobkovsky and P. J. Chirik, *Organometallics*, 2004, **23**, 237.
30 T. J. J. Sciarone, A. Meetsma and B. Hessen, *Inorg. Chim. Acta*, 2006, **359**, 1815.
31 WO Pat., 99/05154, 1999.
32 (a) D. F. Evans, *J. Chem. Soc.*, 1959, 2003; (b) E. M. Schubert, *J. Chem. Educ.*, 1992, **69**, 62.
33 O. Kahn, *Molecular Magnetism*, VCH, New York, 1993.
34 P. Kovacic and N. O. Brace, *Inorg. Synth.*, 1960, **6**, 172.
35 R. J. Kern, *J. Inorg. Nucl. Chem.*, 1962, **24**, 1105.
36 H. L. Lewis and T. L. Brown, *J. Am. Chem. Soc.*, 1970, **92**, 4664.
37 R. R. Schrock and J. D. Fellman, *J. Am. Chem. Soc.*, 1978, **100**, 3359.
38 N. Wiberg and G. Wagner, *Chem. Ber.*, 1986, **119**, 1455.
39 L. Lochmann and J. Trekoval, *J. Organomet. Chem.*, 1987, **326**, 1.
40 J. L. W. Pohlmann and F. E. Brinckmann, *Z. Naturforsch.*, 1965, **20b**, 5.
41 S. Bambirra, D. van Leusen, A. Meetsma and J. H. Teuben, *Chem. Commun.*, 2003, 522.
42 *International Tables for Crystallography*, Kluwer Academic Publishers, Dordrecht, The Netherlands, 1992.